

Prospect Evaluation of Hydrocarbon Reserves Using 3-D Static Modeling in D-Field Onshore, Niger Delta Basin Area

Adekunle O. Sofolabo* Doris Uchechi Akor

Geophysics Research Unit, Department of Physics/Applied Geophysics, University of Port Harcourt, Rivers State, Nigeria

* E-mail of the corresponding author: adekunle.sofolabo@uniport.edu.ng; aosofolabo@gmail.com

Abstract

Qualitative and quantitative approaches are often adopted to characterize known reservoir in any given field. A 3-D static modeling has been used to have full understanding of the field of the reservoir uniqueness of the study area, D-field. The hydrocarbon bearing sounds of the field were modelled using 3-D seismic data of the field, integrating with the well log and checkshot data of the field. The stochastic model approach was adopted to distribute the rock properties (Structural and Petrophysical) into a 3D grid using Sequential Gaussian Simulation which identified fifteen (15) major faults across the reservoirs. Reservoirs R_3000 had average thickness of 123 m, net-to-gross of 65%, porosity of 26%, water saturation of 43%, permeability of 1570.649 mD, based on Rider's classification the reservoir R_3000 shows a very good porosity and an excellent permeability. These values are satisfactory for economic production. The environments of deposition of the reservoirs based on log motifs are interpreted as distributary channel fill and shoreface of the porosity and permeability of D-Field are within the range of values reported in the Niger Delta. Stochastic volumetric analysis estimated that the reservoir of interest to contain a reserve of averagely 14245.50 MMSTB. Furthermore, the integration of these subsurface data (well log and seismic) has led to simulation of a consistent 3-D static model of the reservoir which very well serves as input into the dynamic simulation model, so that forecasting and other sensitivity analysis can be run to provide the basis for effective reservoir management and development strategy.

Keywords: Stochastic model, Qualitative, Quantitative, Gaussian simulation, Static modeling, Volumetric

DOI: 10.7176/JEES/12-3-05

Publication date: March 31st 2022

1. Introduction

With the ever-increasing rate of development and production of oil and gas, one frequently asked question by investors and stakeholders is “when do we run out of oil”? Naturally the hydrocarbon reserves should decrease due to continued increase in production and consumption, but with help of advanced technological skills, reservoirs can be explored and developed and existing fields with compartmentalized reservoirs can be restudied and characterized, to increase the recovery of oil in place (Aly, 1989). The increasing demand for petroleum products has posed a change to the search of oil and gas as the search for hydrocarbon has developed increase with advances in greater computational technology to evaluate the probability of hydrocarbon proneness of the basin thereby limiting the risk factor associated with hydrocarbon (Lukumon, 2014).

It is widely recognized that reservoir characteristics such as: structures, lithofacies heterogeneity, spatial variability of porosity and permeability control the reservoir performance, development strategies and the returns on investment on the reservoirs (Ailin and Chengye, 2012). Reservoir characterization is the process of describing various reservoir characteristics such as geologic, petrophysics, geochemical and engineering properties. It also involves, using all available data to provide reliable reservoir models for accurate reservoir production and performance prediction, in addition to providing economic and quality decision making in order to determine the viability of the reservoir(s) under study (Jong-Se, 2005). The 3-D reservoir model is a computational and geological model of a petroleum reservoir displaying the spatial representation of the reservoir properties, captured key heterogeneity of the reservoir. The purposes of modeling a reservoir is to improve estimation of reserves and make decisions regarding the development of the field while evaluating alternative reservoirs. Integrated reservoir models represent the most valuable technical approach for estimating the oil and gas reserves and computing profiles, reducing the uncertainties always associated with the reservoir volume and description (Toba, 2017).

1.1. Location of The Study Area

The study area is located at D-Field, within the onshore area of Niger Delta in Nigeria (Figure 1). The terrain is generally swampy in nature, with river channels and tributaries emptying into the Atlantic Ocean. The Field lies between longitude 6°17'55'E and latitude 4°37'27'N. The Field is located within the Central Swamp Depobelt, Onshore Niger Delta.

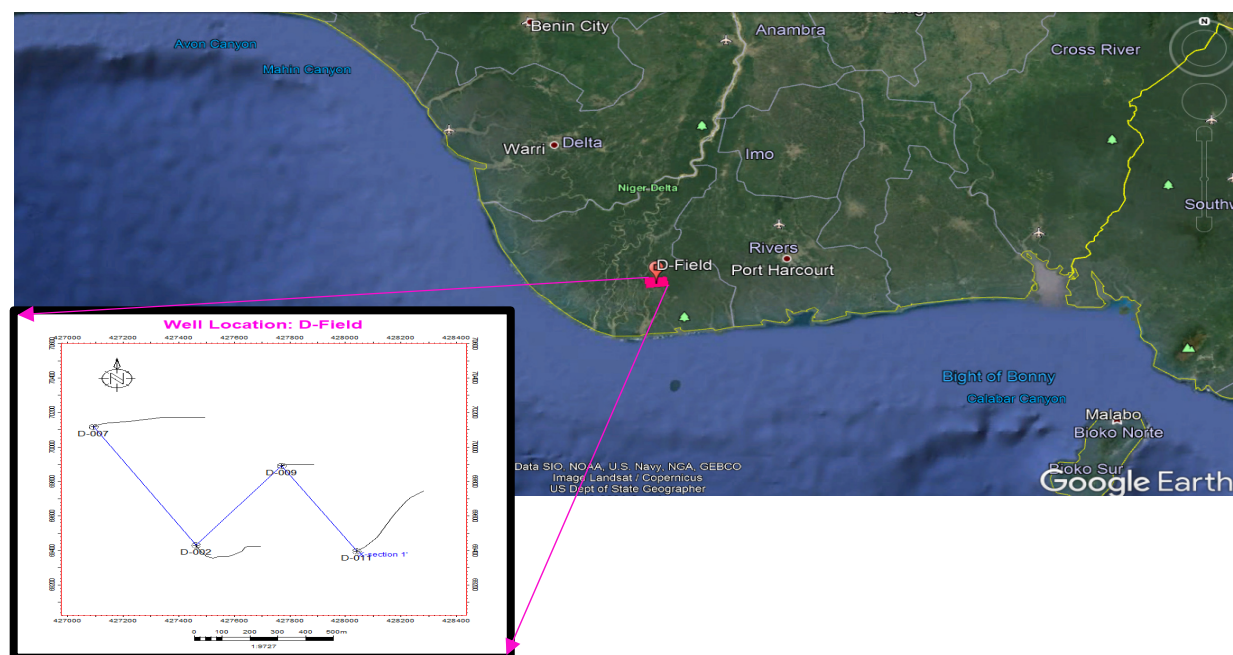


Figure 1: A map showing the location of the D-Field, Onshore Niger Delta (Source: Google Earth 2021) and the Base map for D-Field showing the distribution of wells within the area.

1.2. GEOLOGICAL FRAMEWORK OF THE STUDY AREA

Structural Overview of Niger Delta Basin

The studied area Field lies in the Niger Delta petroliferous basin, a productive hydrocarbon area in the Gulf of Guinea, southern Nigeria. The northern part of the boundary at 300,000 km² Niger Delta Province is the Benin flank, an east-northeast trending hinge line south of the West Africa basement massif. Outcrops of the Cretaceous on the Abakaliki High define the northeastern boundary. The east-southeast edge is outlined by the Calabar flank- a hinge line bordering the adjacent Precambrian. The Niger Delta oil and gas province is situated in the Gulf of Guinea on the west coast of Central Africa (Figure 2), and extends entirely over the Niger Delta zone (Stacher *et al.*, 1995). The Niger Delta consists of a generally regressive clastic succession that is 10 - 12 km thick. The field comprises a single recognized petroleum system, which is the Tertiary Akata - Agbada petroleum system (Figure 3). While the boundaries of the province coincide with the maximum extent of the system, the minimum petroleum system is well defined by oil and gas field center points. The Tertiary classification of Niger Delta is subdivided into three large stratigraphic parts (Figure 4) namely: Akata, Agbada, and Benin Formations in the downward direction of sedimentation. The basinward decrease in age reflects the overall regression of environments of deposition within the Niger Delta clastic wedge province. These Formations show a massive coarsening-upward progradational clastic wedge (Short and Stauble 1967) deposited in fluvial, deltaic, and marine environments (Weber 1986; Weber and Daukoru 1975).

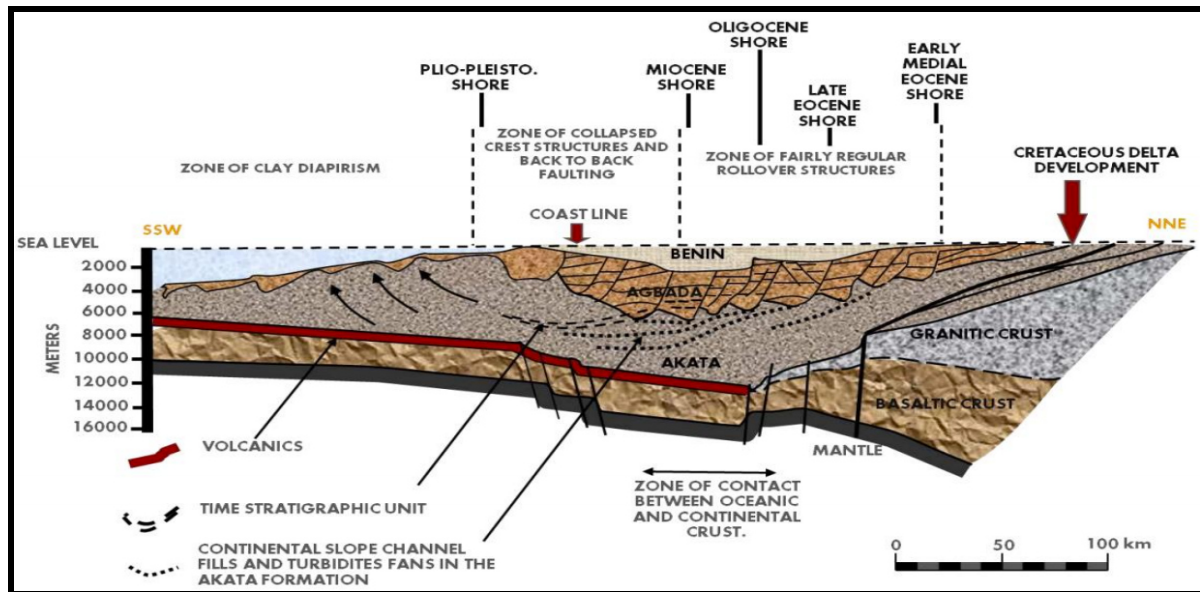


Figure 3: Schematic Dip Sections of the Niger Delta structures and traps (Weber and Daukoru, 1975)

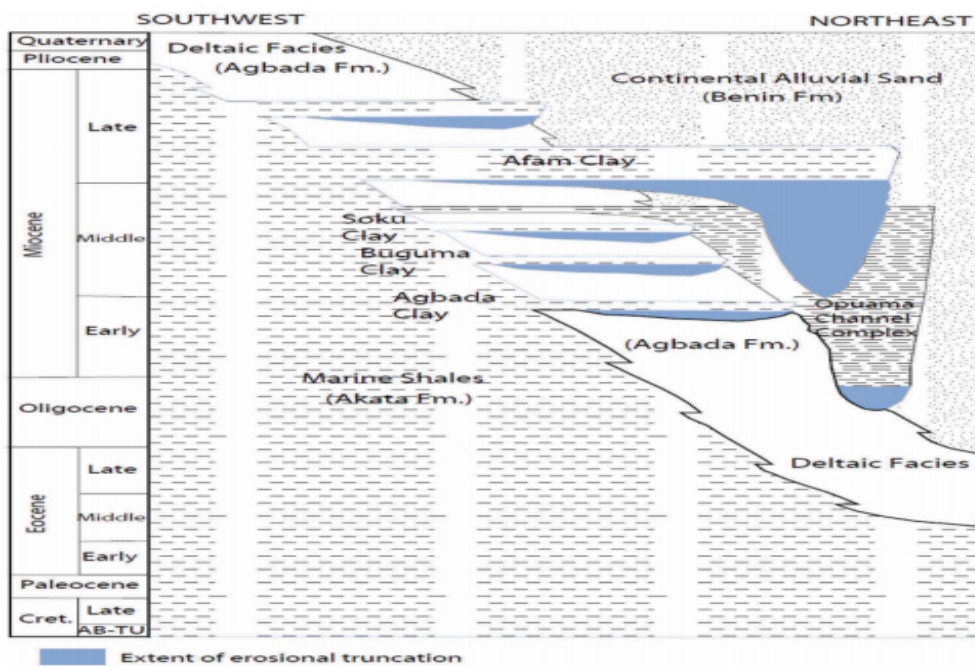


Figure 4: Stratigraphic column of the three formations in Niger Delta. (Shannon and Naylor 1989).

2. Materials and Methods

2.1. Materials

This study was conducted using 3-D seismic data and well log obtained from D-field, onshore Niger Delta Area (study area). Some of the available data in the well log suite, comprises of Gamma ray (GR) logs, Caliper logs, Porosity logs (neutron, density and sonic) and resistivity (shallow and deep) with their well header information, check shot data and well survey deviation data. The seismic data utilized was a processed post-stack 3-D seismic section, with wavelet that is zero phased, having SEG reverse polarity 5577 - 5850 inlines and crosslines 1495 - 1750, with line spacing of 25 meters.

Schlumberger PETREL™ (2017 version) Software was used for loading the post-stacked 3-D seismic volume and well log data, data appraisal, petrophysical analysis, well correlation, well to seismic tie, seismic interpretation, fault modeling, pillar gridding, horizon, zone, and layering making, well logs scale up, data analysis, petrophysical modeling, and generation of hydrocarbon prospect maps.

2.2. Methods

The following methods outline below was adopted for the study, the outlined procedures shows a detailed steps in building the static (earth) model for the reservoir of interest. These steps are

1. Data gathering and data loading into industry-based software.
2. Data QC
3. Well logs conditioning
4. Well Log Correlation.
5. Petrophysical Evaluation.
6. Seismic data pre-evaluation and reflective pattern analysis.
7. Seismic Interpretation
8. Synthetic seismogram generation, well to seismic tie and phase determination.
9. Velocity Modeling
10. Static Modeling (Structural and Property Modeling)
11. Static Volume Estimation and Evaluation
12. Hydrocarbon Prospect evaluation

2.3. Research Workflow

The process for the 3-D reservoir modeling requires input from Geophysical, Geological and Petrophysical data. The static model in turn serves as input for the Reservoir Engineer (RE) to build the dynamic model. Figure 5 shows the workflow used for this study.

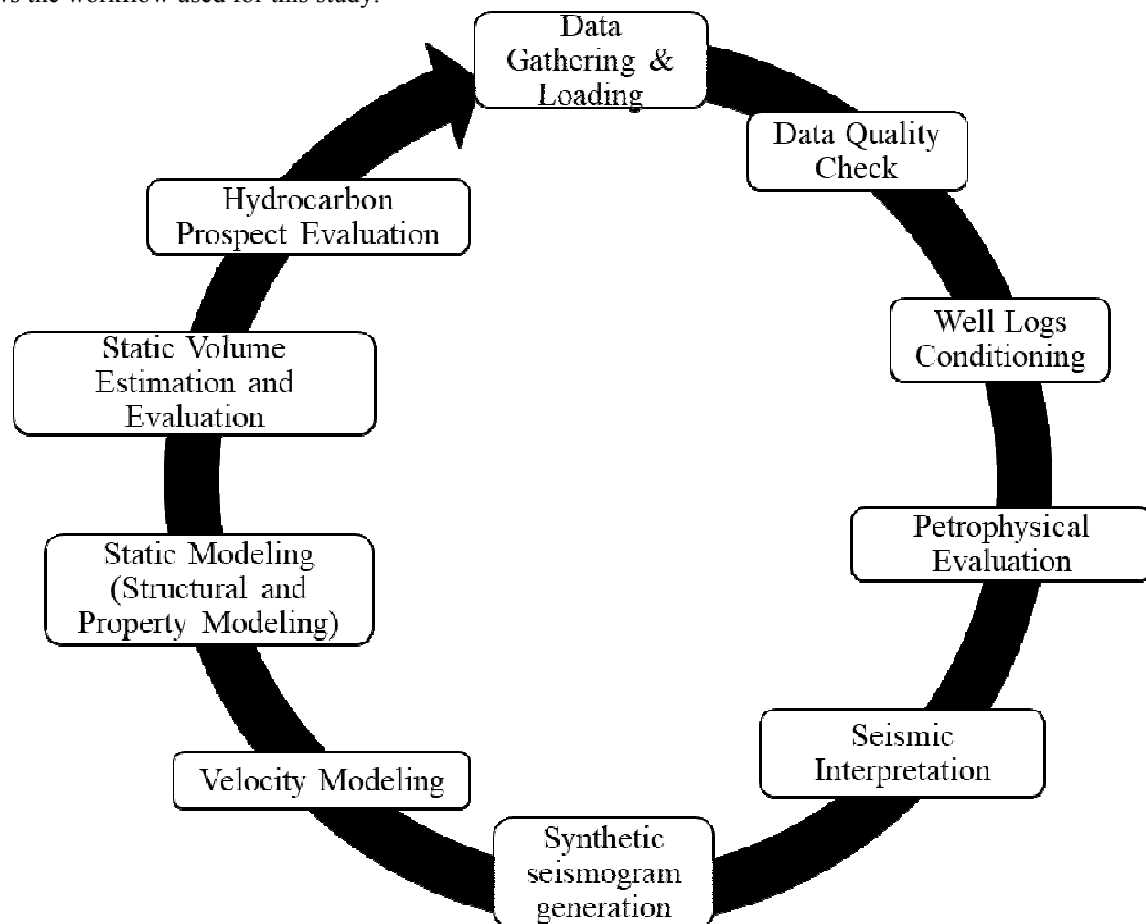


Figure 5: Integrated Workflow utilized for the analysis of D-Field

2.3 Well Information

The data were loaded into the software using necessary well information such as well header, deviation, well datum as well as geographical references. A total of 4 wells were available and utilized for this study which included: D-002, D-007, D-009, and D-011. All well logs were provided in meters. Only well D-011 had checkshot provided. A table of information used is shown in Table 1.

WELL LOGS									
WELL NAME	Gamma Ray	Caliper	Resistivity	Density	Neutron	Sonic	Well Header	Checkshot	Directional survey
D-002	A	A	A	A	A	A	A	NA	A
D-007	A	A	A	A	A	A	A	NA	A
D-009	A	A	A	A	A	A	A	NA	A
D-011	A	A	A	A	A	A	A	A	A

LEGEND: A – AVAILABLE, NA – NOT AVAILABLE

2.4 Well Log Correlation

The well logs were utilized to define the reservoir sands and qualitative interpretations were carried out using a quick look approach. This enabled the identification of the lithology of the formation using gamma ray log and resistivity logs and fluid discrimination using the neutron density crossplot. In the quick look approach for qualitative interpretation, the lithology was recognized through the definition of shale baseline, high gamma ray log values depict non-permeable bed, (shale) and low gamma ray log values identified the permeable beds (sandstone). Comparison of the low gamma ray log value to a high resistivity reading from the resistivity log showed a probable hydrocarbon-bearing sand unit. This quick look quantitative interpretation of the well log signatures revealed numerous reservoir sand units (Figure 6) while the well correlation showed the reservoir heterogeneity and continuity of the sand bodies across the four well provided.

The following petrophysical properties were evaluated for the reservoirs of interest for the different wells in the field of study, namely shale volume, permeability, porosity (effective and total), fluid saturation (water and hydrocarbon) and net-to-gross, using standard Petrophysical equations. Full volume 3-D seismic interpretation was adopted to infer high resolution seismic stratigraphy, the full variability of depositional system was used to obtain true seismic and sequence stratigraphic interpretations at high frequency. Geological fault interpretation was picked at 5 slice intervals, on the inline and arbitrary lines were taken where the fault pattern did not show clearly. Major and minor discontinuities on the seismic lines were identified and picked. Seismic attribute in the form of variance attribute was applied to enhance seismic amplitudes to be good enough and discontinuities were clearly found around the central part of the seismic data, this revealed structural deformations visibly, this aided the identification and mapping of faults on the time slices, before the faults mapped were extended on the inline section of the seismic data. These identified faults were assigned names, colour-coded and correlated. Having tied seismic to well data, reservoir time horizon was identified, picked, and interpreted. Horizon interpretation was picked at 5 x 5 grid intervals for the in-lines and cross-lines due to structural complexity of the field (Figure 8). Structural smoothening was utilized to enhance the visibility and continuity of seismic events which aided horizon interpretation.

The checkshot available for well D-011 was calibrated to the sonic log in order to realign the sonic log. The result of the calibrated sonic log, the density, and Ricker wavelet of 25 Hz were utilized in generating the synthetic seismogram. The synthetic seismogram was generated using acoustic impedance log (AI) and reflective coefficient log (RC), while the original seismic was correlated with the synthetic seismogram and the characteristics of the wavelet (wavelet, power and phase spectrum) was modelled as the seismic trace which is the representative of the well in 1-D in form of the seismic data.

2.5 MODELING

2.5.1 Velocity Modeling and Depth Conversion

The Time Depth Relationship (TDR) velocity function generated from the seismic-to-well tie was employed for depth conversion. This function was displayed as a graph of time way travel time (TWT) versus depth in Petrel and various polynomial functions were tested to find a good fit (Figure 10).

2.5.2. Static Modeling

The static or geological modeling procedure was performed to combine the structural and property models in forming a single model. This model uses geological concept to describe the architecture of fluid flow pathways within the reservoir (static reservoir model). Structural model comprises of fault modeling, horizon modeling and 3-D gridding while property model comprises of facies modeling and petrophysical modeling. The model in which the fault pillars was defined and the faults model generated, which was used to produce the 3-D grid model of the reservoir. Then, the depth-converted horizons/surfaces were inserted into the 3D grid, producing horizon models fitting the defined model boundary. The structural modeling method employed ultimately created a structural 3-D grid housing the three reservoirs

The grid cells generated was then populated with the facies and petrophysical properties, resulting in a model more representatives of the subsurface; the estimated petrophysical properties from the 1-D well logs were upscaled, analyzed and then populated across the created model. A variogram is used to model the way in

which two values in space or time are correlated, giving a quantitative description of the variation in a property as a function of the separation distance between data points

2.5.3. Petrophysical Modeling

Petrophysical analysis was done to interpret the data properties such as shale volume, permeability, porosity (effective and total), water saturation and net-to-gross (Petrophysical modeling) using the Gaussian Random Function Simulation (GRFS) algorithm, this is also known as stochastic technique.

2.5.4. Static Volume Estimation and Evaluation

The volumetric of the hydrocarbon reserve in the field was calculated using the static model of the field, which comprises of the structural model and property models, combine with the petrophysical model built, to estimate the reserves in terms of stock tank of original oil in place (STOIIP) of the reservoir. The estimation of the STOIIP within the reservoir was done using the 3-D grid of the petrophysical averages. Five case of the reservoir STOIIP were simulated and estimated using the averages porosity value, water saturation and Net-To-Gross. This was combined with the formation volume factor ($B_o = 1.65$) and the actual recovery factor (RF) to estimate the STOIIP.

3. Results and Discussion

3.1. Results

The results of this study are presented as follows; well log evaluation of the available wells, well correlation, petrophysical properties analysis, seismic interpretation, and 3D static modeling of petrophysical properties estimated for the reservoir. The lithology correlation of the wells is shown in Figure 6, while the individual petrophysical properties of the wells are shown in Figure 7 and 8 respectively. A combined correlation of the well showing the five delineated reservoirs is shown in Figure 9.

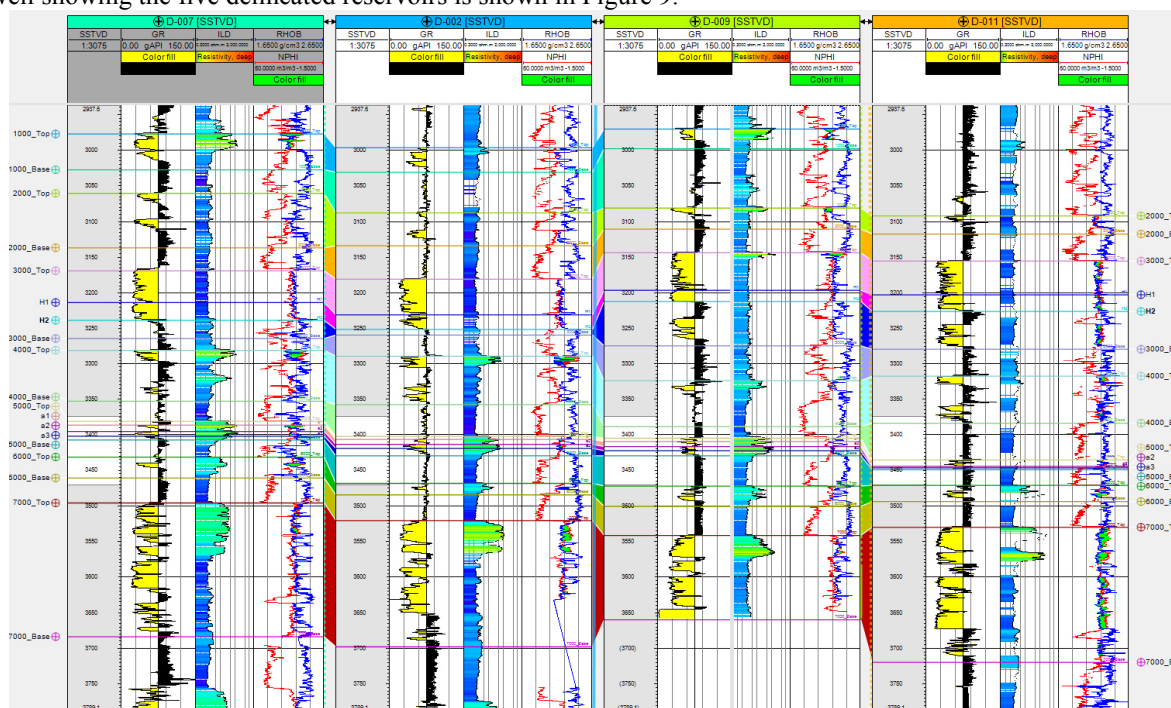


Figure 6: Lithological Well Log Correlation of Reservoir in D-Field

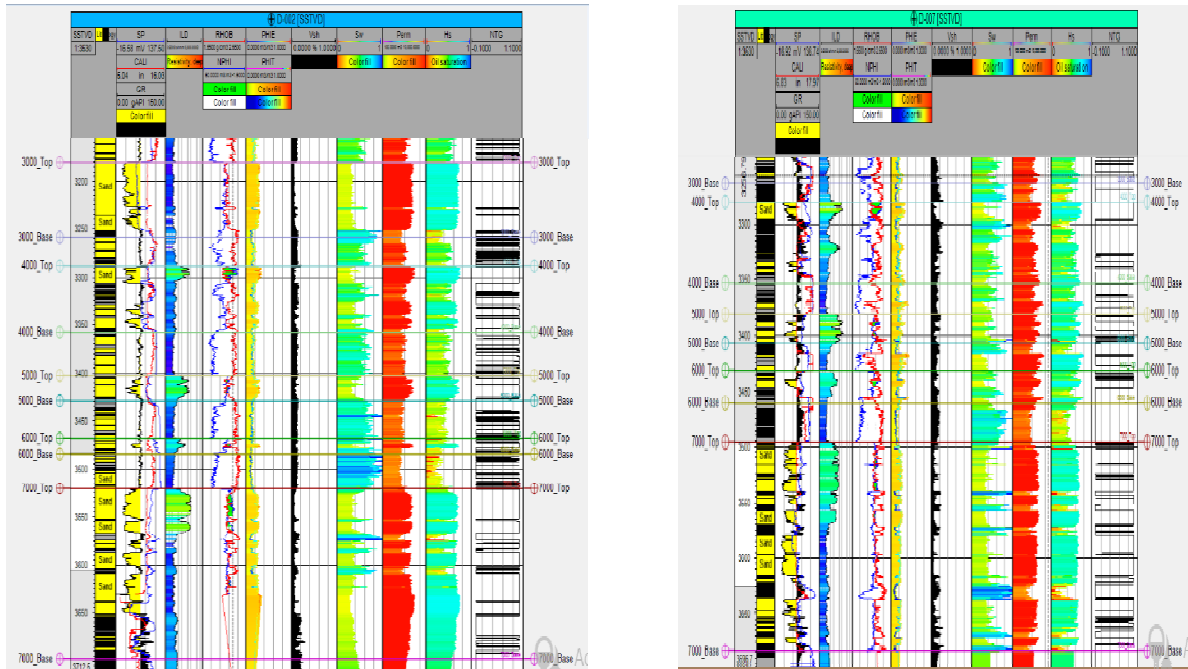


Figure 7: Correlated petrophysical properties of (a) Well D-002 and (b) Well D-007

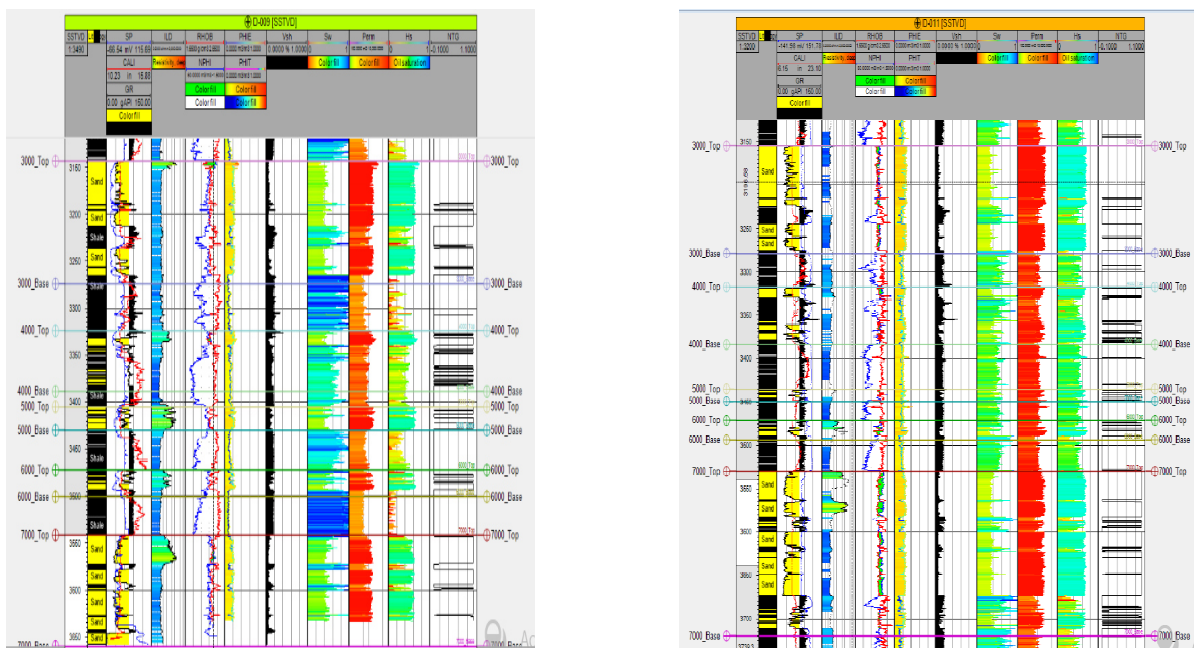


Figure 8: Correlated petrophysical properties of (a) Well D-009 and (b) Well D-011

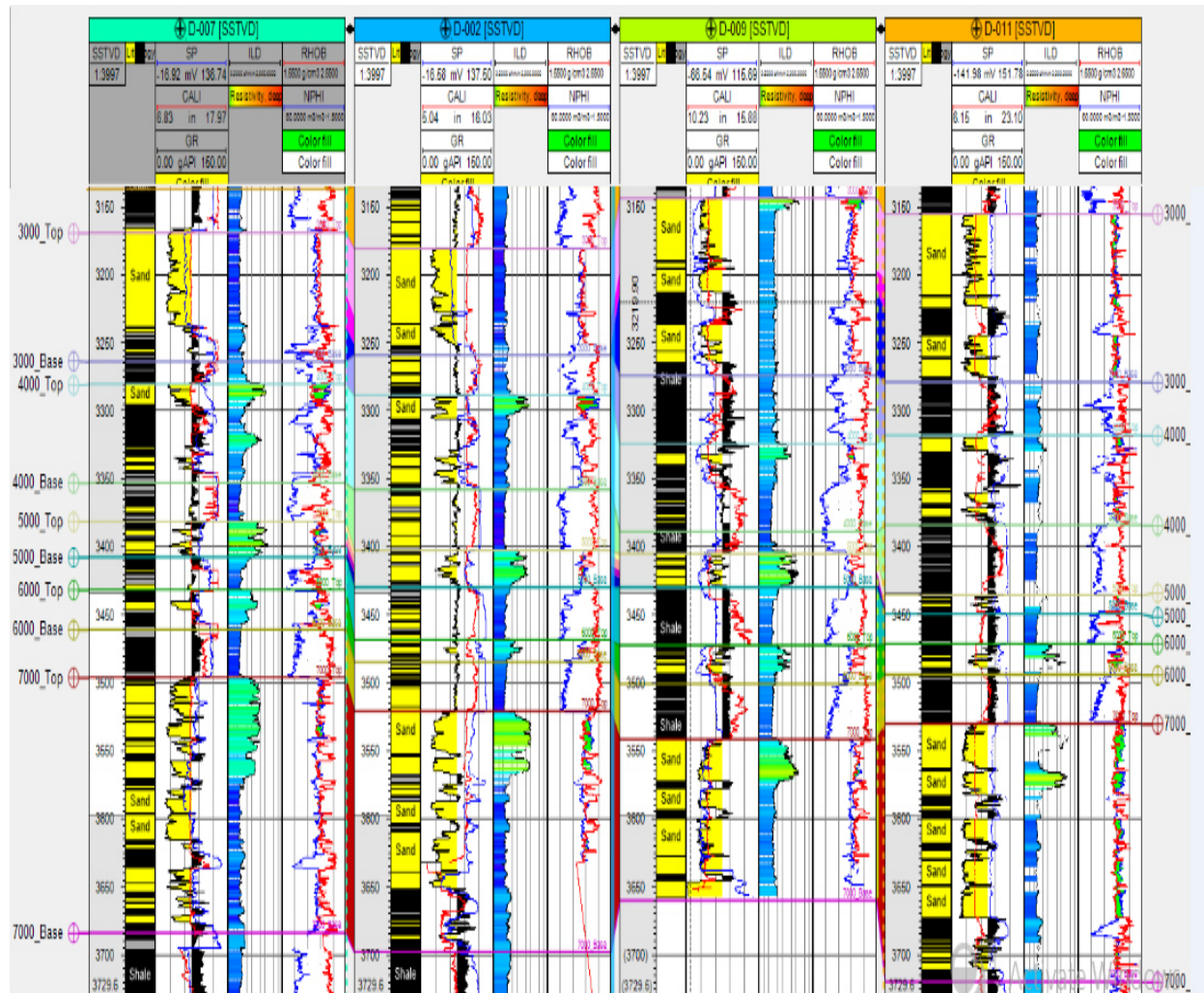


Figure 9: Lithology correlation of the five reservoirs delineated across the four wells in the Field.

The results of the petrophysical properties estimated from the delineated reservoirs across the four wells are presented in Table 2. The seismic interpretation was used to map the faults and the horizons. Variance attribute was applied to the seismic volume, to enhance fault traces, a total of 15 faults were interpreted, both synthetic (growth faults) and authentic fault structures were mapped, and this helped to delineate hydrocarbon prospects. Horizons were picked after the results of the seismic to well confirm the accurate placement of the well top for reservoir R_3000 of interest (Figure 10 and 11). The seismic to well tie result used is shown in Figure 12

Table 2: Petrophysical parameters estimated for the delineated reservoir units in the four wells.

Wells	Reservoir sands	Top (m)	Base (m)	Gross thickness (m)	Shale volume (%)	Shale volume (m)	Net sand (m)	Net-to-Gross (%)	Total Porosity (%)	Effective Porosity (%)	Water saturation (%)	Permeability (mD)	Hydrocarbon saturation (%)	Fluid type
D-002	R_3000	3180.75	3258.56	77.81	13%	10.1153	67.6947	87%	23%	22%	45%	1845.389	55%	Oil/Water
	R_4000	3289	3358	69	14%	9.66	59.34	86%	22%	20%	59%	1744.303	41%	Oil/water
	R_5000	3402	3431	29	12%	3.48	25.52	88%	19%	17%	56%	1155.55	44%	Oil/Water
	R_6000	3469	3485	16	12%	1.92	14.08	88%	13%	11%	82%	691.9105	18%	Oil/Water
	R_7000	3521	3698	177	13%	23.01	153.99	87%	20%	19%	78%	1636.715	22%	Oil/Water
D-007	R_3000	3135.84	3259.9	124.06	15%	18.609	105.451	85%	27%	26%	42%	1789.458	58%	Oil/Water
	R_4000	3280	3352	72	17%	12.24	59.76	83%	24%	22%	42%	1540.439	58%	Oil/Water
	R_5000	3381	3407	26	14%	3.64	22.36	86%	25%	21%	52%	1821.868	48%	Oil/Water
	R_6000	3431	3460	29	13%	3.77	25.23	87%	28%	25%	41%	2019.133	59%	Oil/Water
	R_7000	3496	3684	188	14%	26.32	161.68	86%	26%	22%	82%	2214.002	18%	Oil/Water
D-009	R_3000	3142.54	3275.76	133.22	15%	19.983	113.237	85%	23%	22%	44%	2001.674	56%	Oil/Water
	R_4000	3325	3389	64	23%	14.72	49.28	77%	25%	23%	35%	2037.376	63%	Oil/Water
	R_5000	3404	3430	26	13%	3.38	22.62	87%	19%	17%	66%	1254.444	34%	Oil/Water
	R_6000	3472	3501	29	14%	4.06	24.94	86%	15%	14%	56%	1001.586	28%	Oil/Water
	R_7000	3542	3660	118	13%	15.34	102.66	87%	15%	14%	76%	995.2449	24%	Oil/Water
D-011	R_3000	3205.08	3283.56	78.48	14%	10.9872	67.4928	86%	24%	23%	45%	1389.078	55%	Oil/Water
	R_4000	3318	3384	66	30%	19.8	46.2	70%	19%	16%	78%	1313.773	22%	Oil/Water
	R_5000	3435	3449	14	15%	2.1	11.9	85%	19%	16%	51%	991.2469	49%	Oil/Water
	R_6000	3471	3494	23	14%	3.22	19.78	86%	29%	24%	44%	2276.725	56%	Oil/Water
	R_7000	3531	3720	189	16%	30.24	158.76	84%	19%	17%	81%	1434.346	19%	Oil/Water

3.2. Surface Generation

The surfaces maps were generated using the seed grid (Figure 13) for reservoir R_3000. The time surfaces (time structure map) and the depth surfaces (depth structure map) generated for reservoir R_3000 using the seed grid are shown in Figure 14 and 15. There was a significant difference in structures on the time surfaces and the depth

surfaces, indicating that the velocity function (Figure 16) used for depth conversion is good. The time to depth conversion surface maps generated is shown in Figure 17.

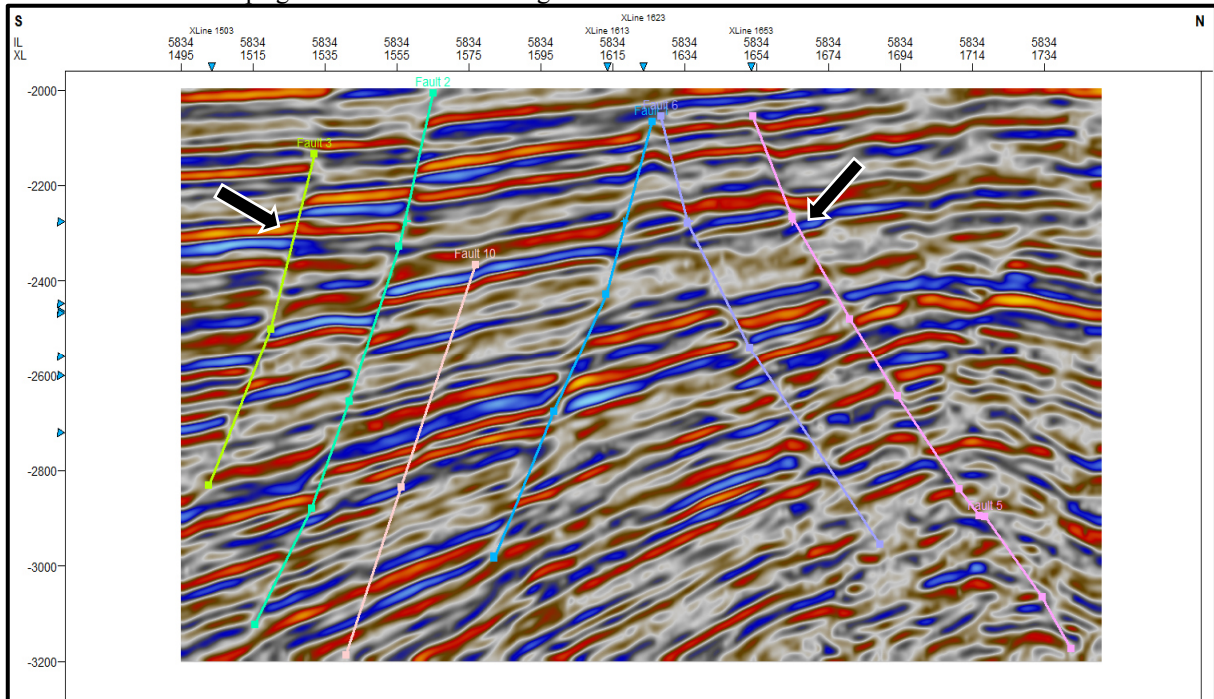


Figure 10: Seismic section showing the interpreted faults of interest.

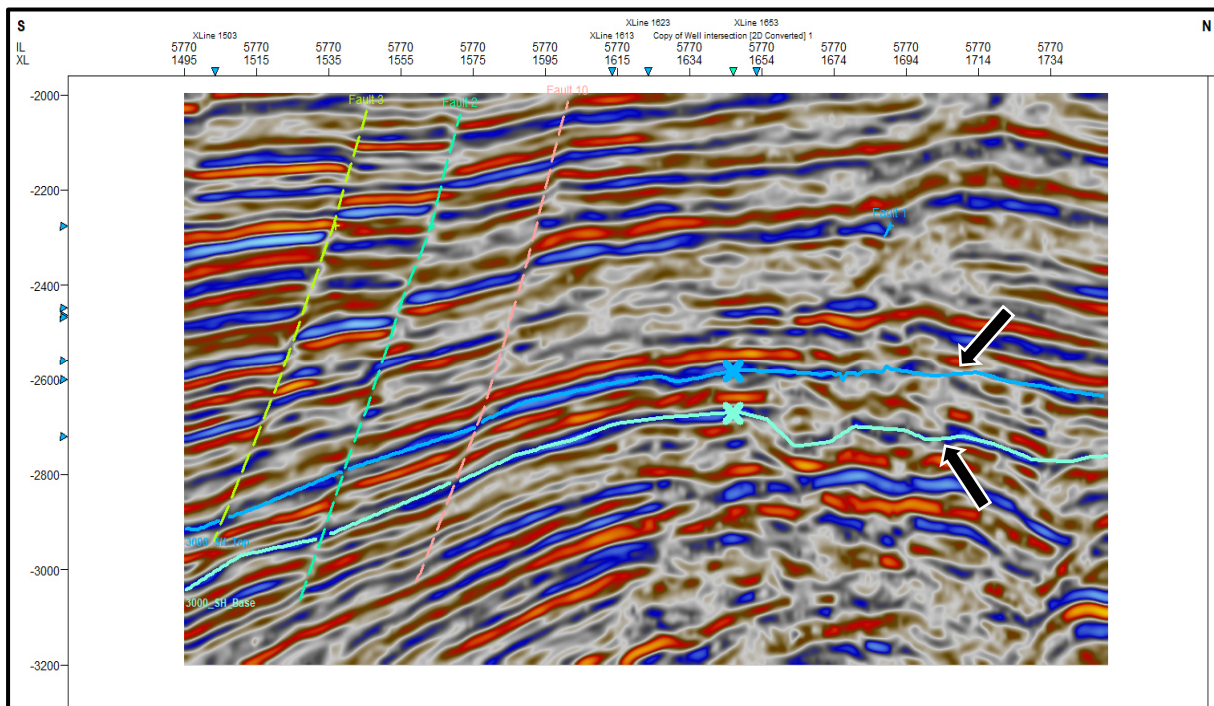


Figure 11: Seismic section showing the interpreted horizons of interest

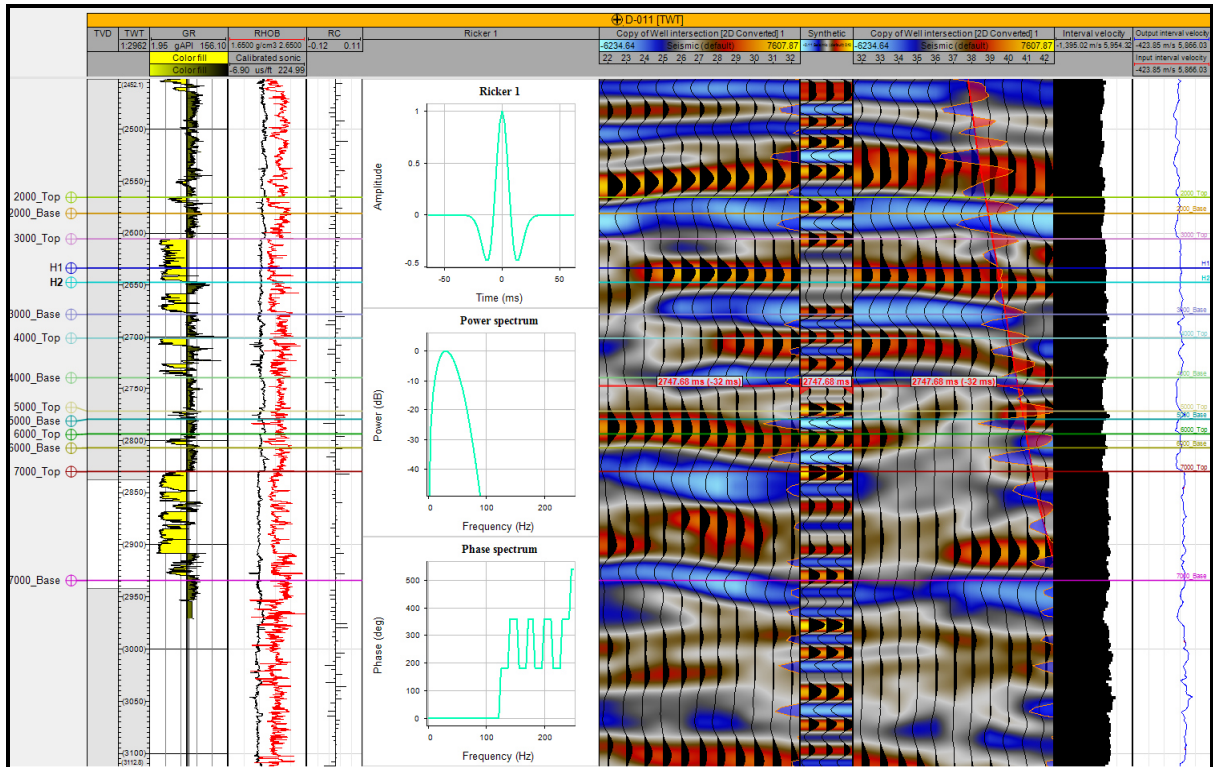


Figure 12: Seismic to well tie for Well D-011

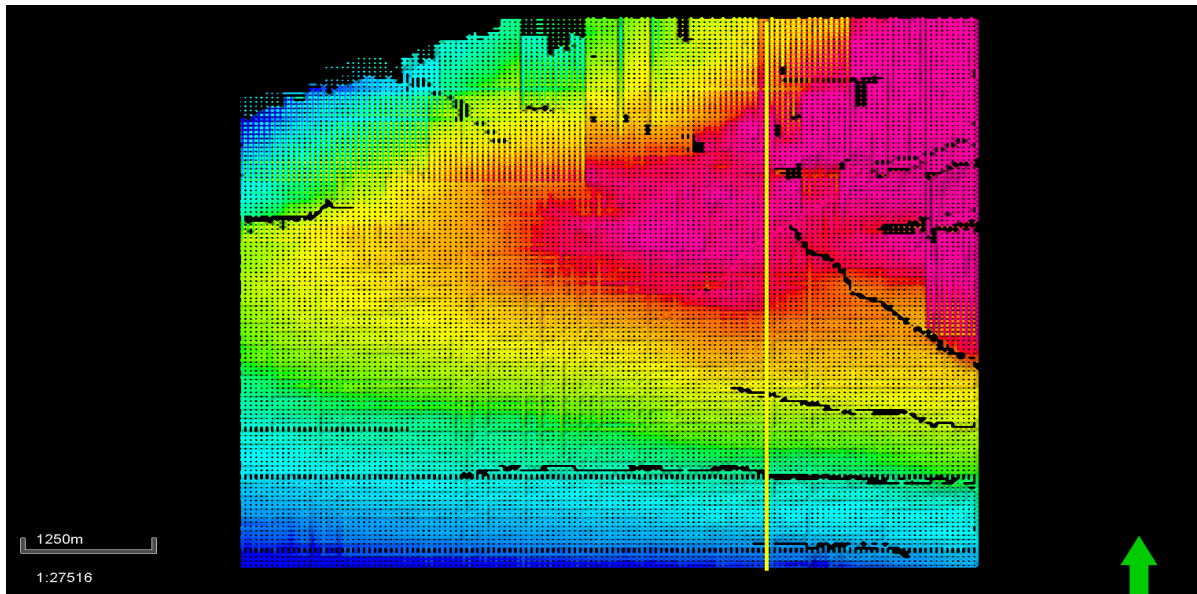


Figure 13: Mapped 3D seed grid for the R_3000 top

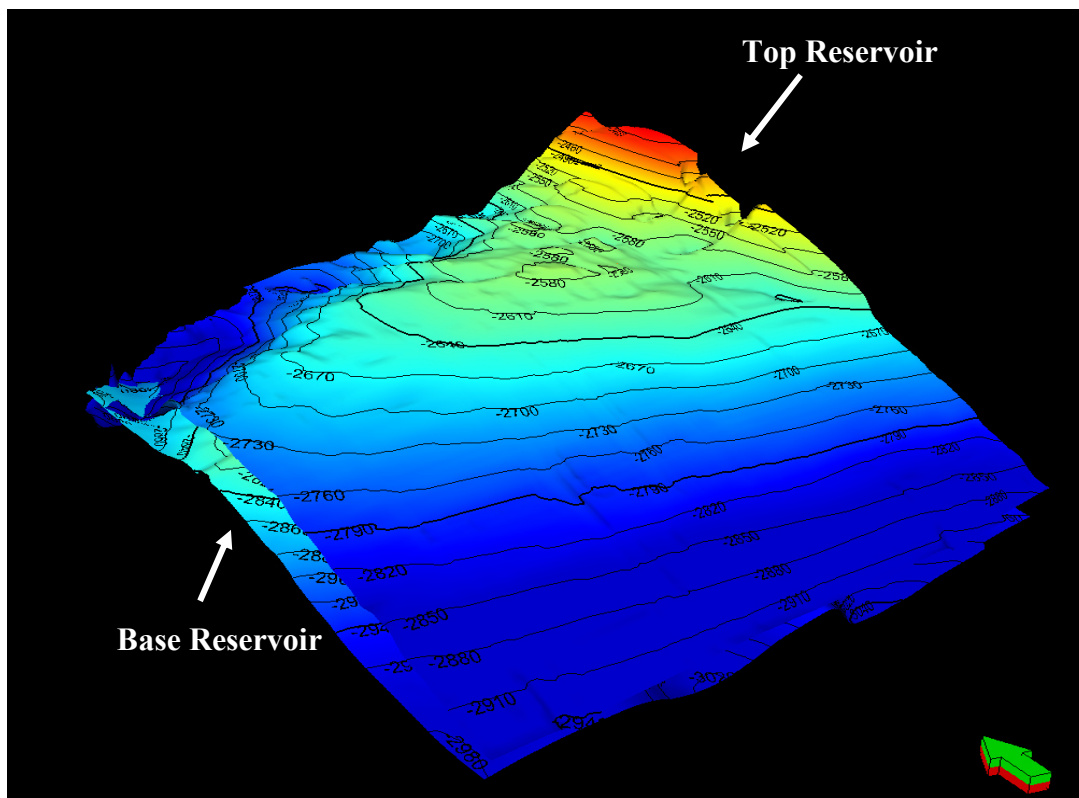


Figure 14: Time Surface map showing top and base for reservoir R_3000

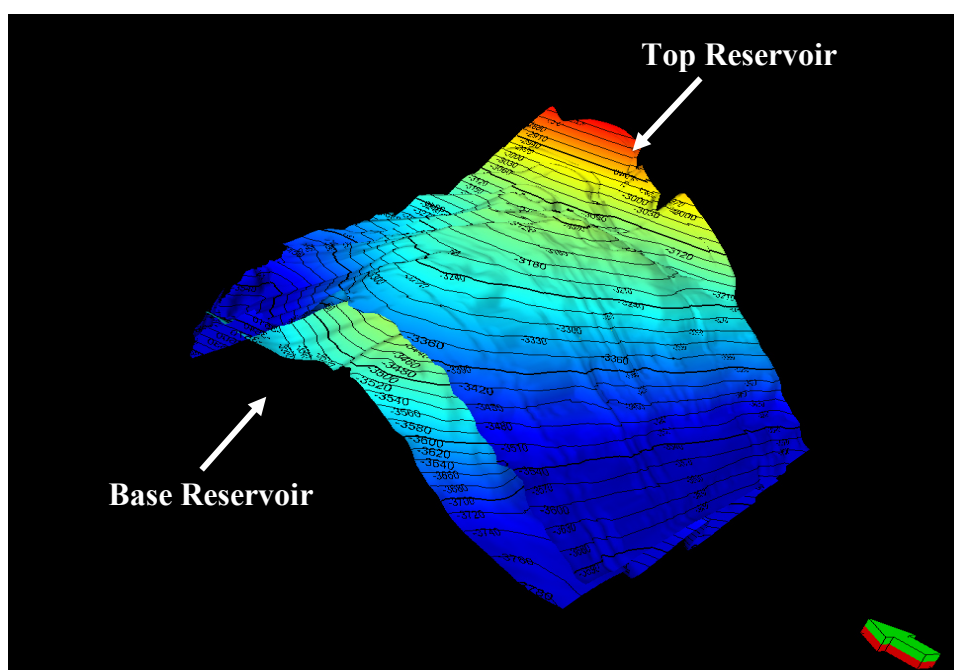


Figure 15: Depth Surface map showing top and base for reservoir R_3000

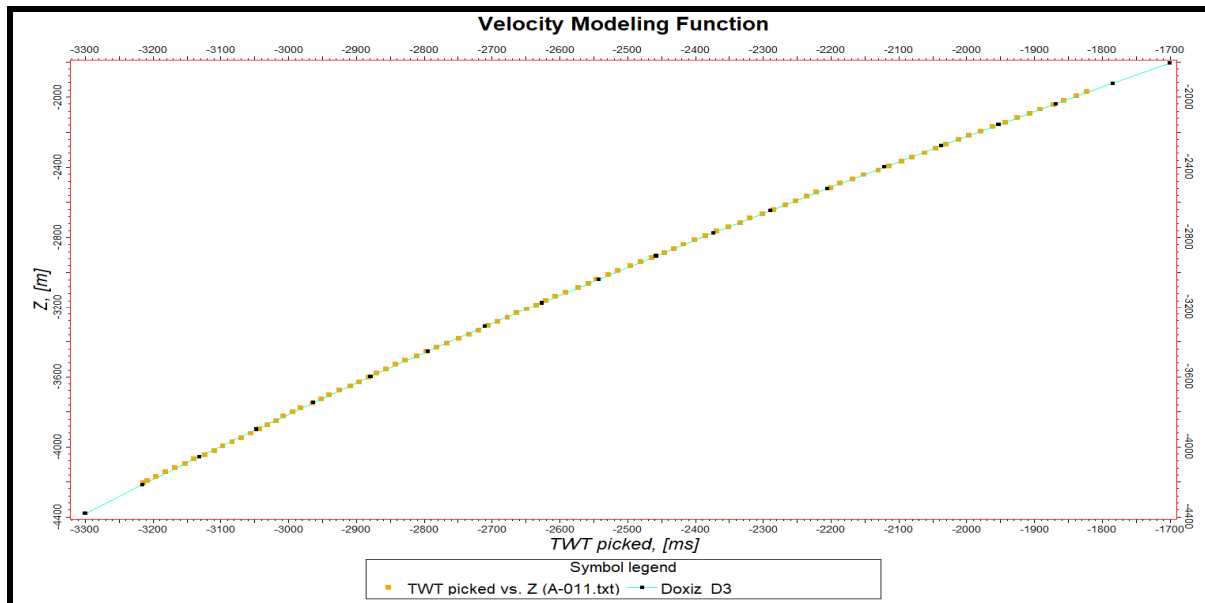


Figure 16: Velocity Modeling Function generated used for the time depth conversion

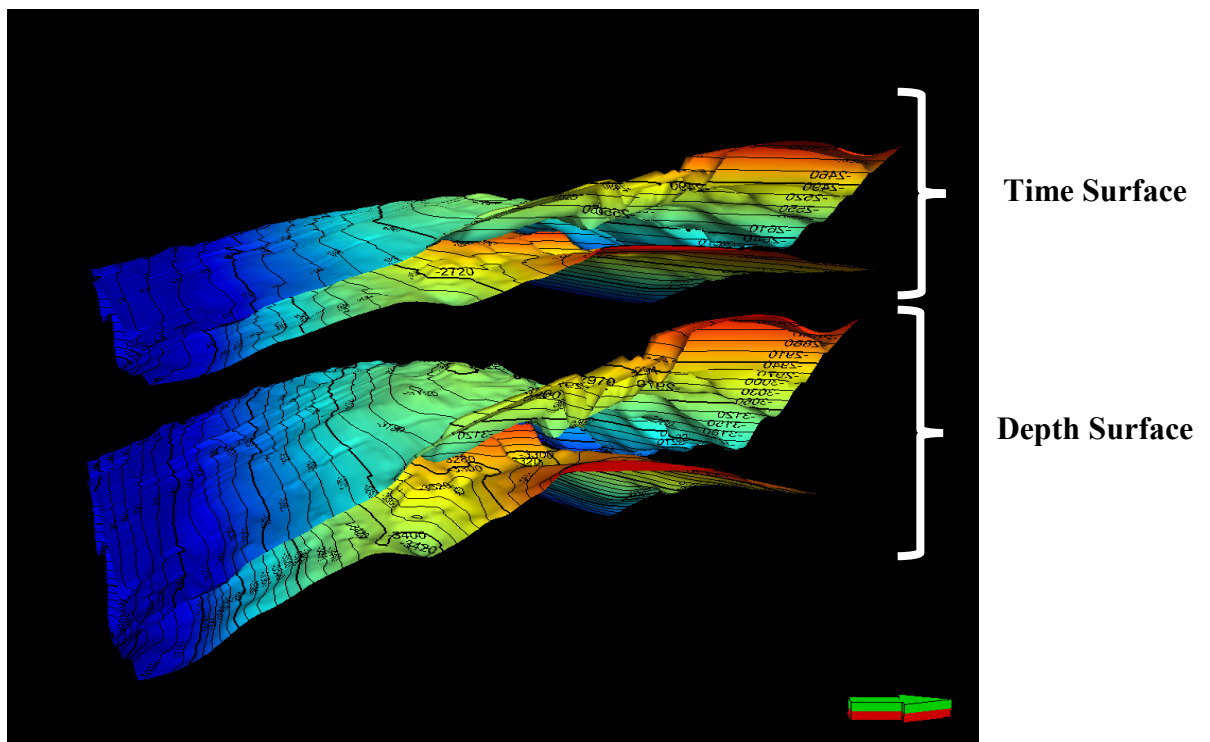


Figure 17: Conversion of the time surface map to depth surface map after applying the velocity function.

3.3. 3-D Static Modeling

Fault pillars were generated from the fault sticks, the pillars were later converted into faults plane, which was used to modelled the faults (Figure 18). The modelled faults were used to generate the 3-D grid showing the modeled faults for reservoir R_3000 as shown in Figure 19. The result of the pillar gridding section was visualized on the 2D window of the interpretational tool revealing grid cells for the model simulated (Figure 20). Visualization of the horizon modelled, zoning and layering resulted in the simulation of the reservoir subsurface, R_3000 as shown in Figure 21.

3.4. Petrophysical Modeling

The 3-D petrophysical models was used to visualized the result of the generated petrophysical properties for reservoir R_3000 of the field, the corresponding model generated includes; Shale Volume (Figure 22), Net to Gross (Figure 23), Effective and total porosities (Figure 24 and 25), Permeability (Figure 26) and Water

Saturation (Figure 27) respectively. From the petrophysical models of the properties, the oil-water contact model was generated (Figure 28), which is an important parameter for the volumetric estimation and calculation of the oil in place. The results obtained from the generated models was used to stimulate a five case scenarios for the STOIIP in the reservoir of interest, R_3000 and the results obtained is shown in Figure 29.

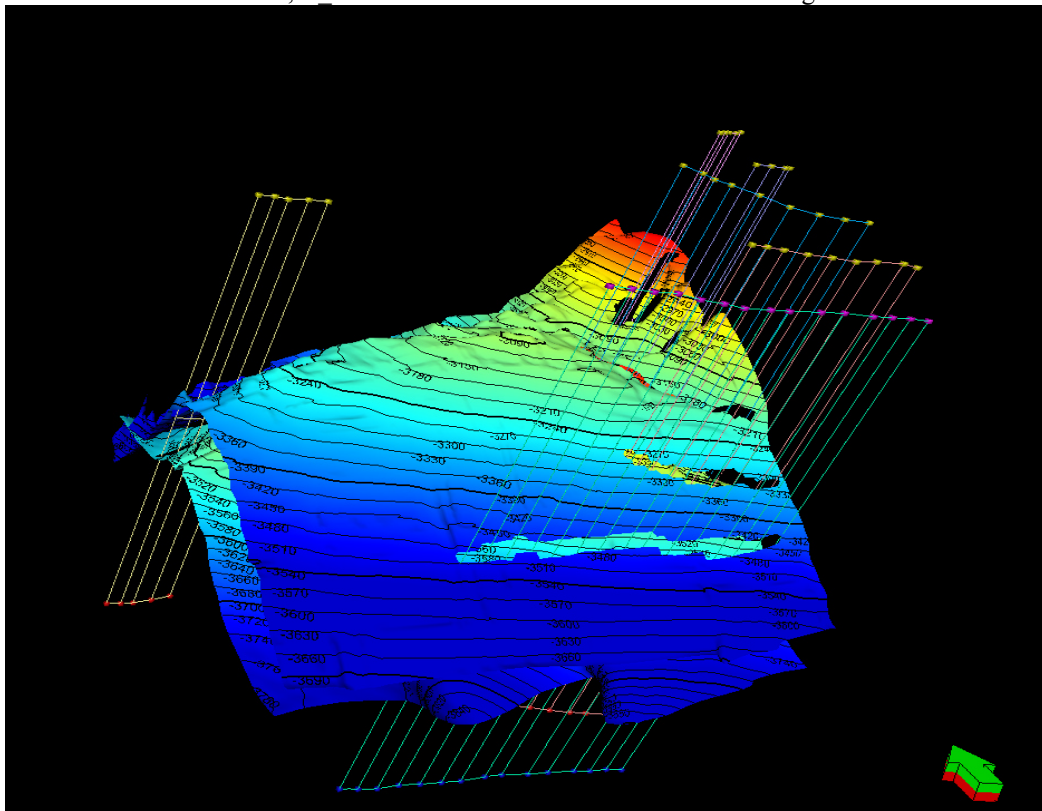


Figure 18: Fault modeling with its associated fault pillars for reservoir R_3000

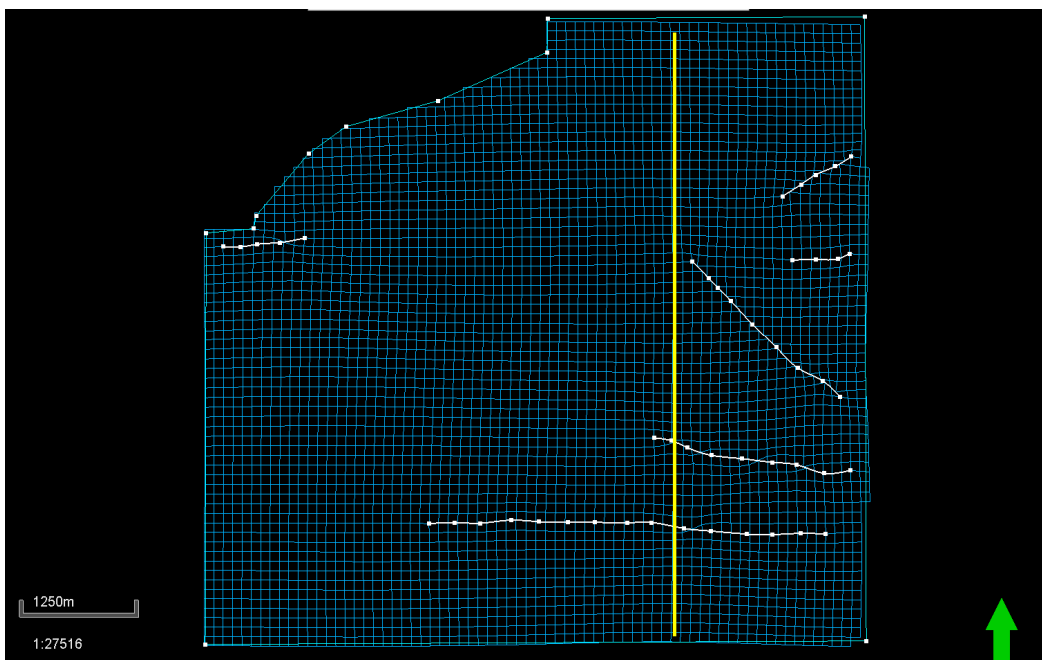


Figure 19: Pillar gridding showing modelled faults for reservoir R_3000

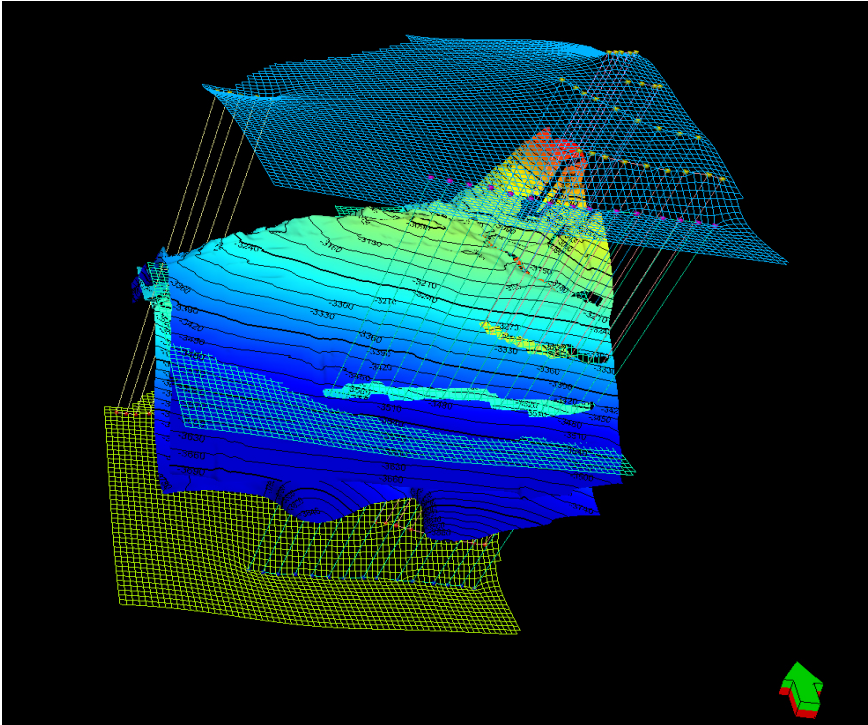


Figure 20: 3D Pillar grid for indicating top, mid and base skeleton

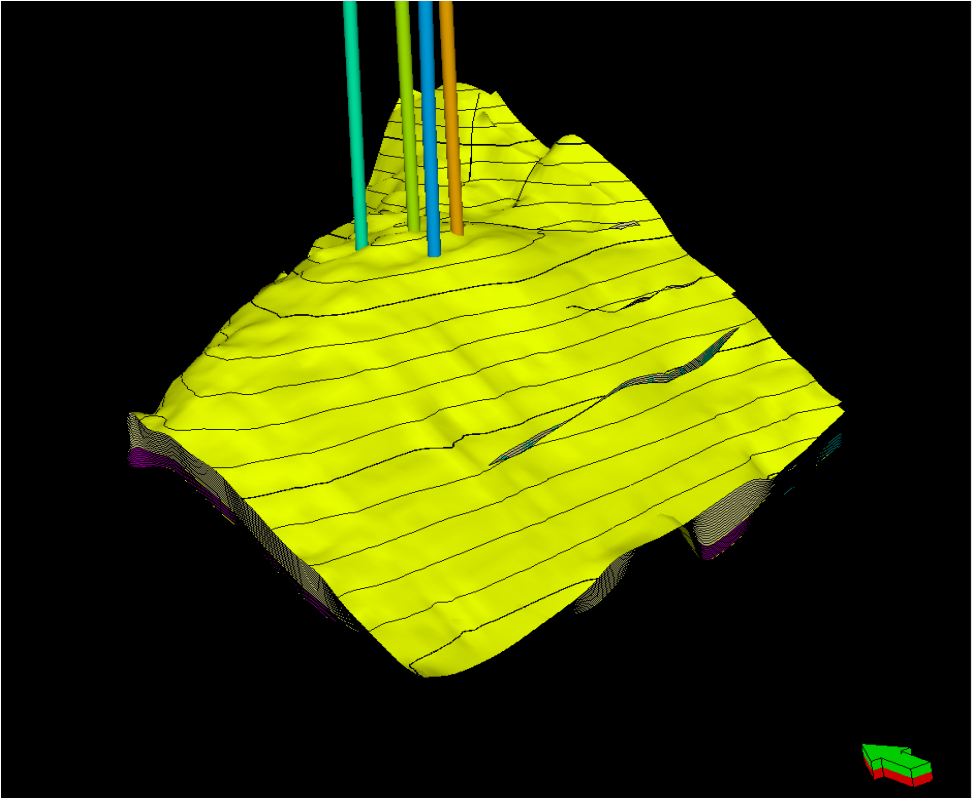


Figure 21: Horizon modelled, zone and layering generated

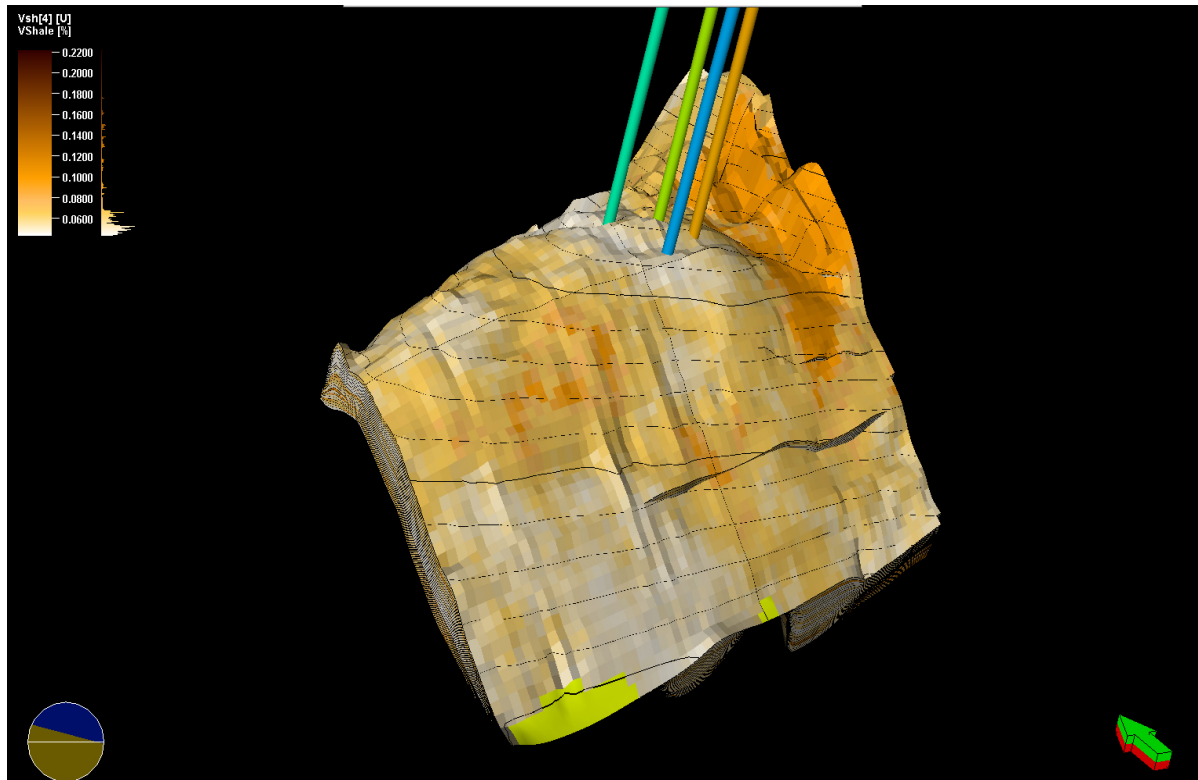


Figure 22: Shale volume model generated for reservoir R_3000

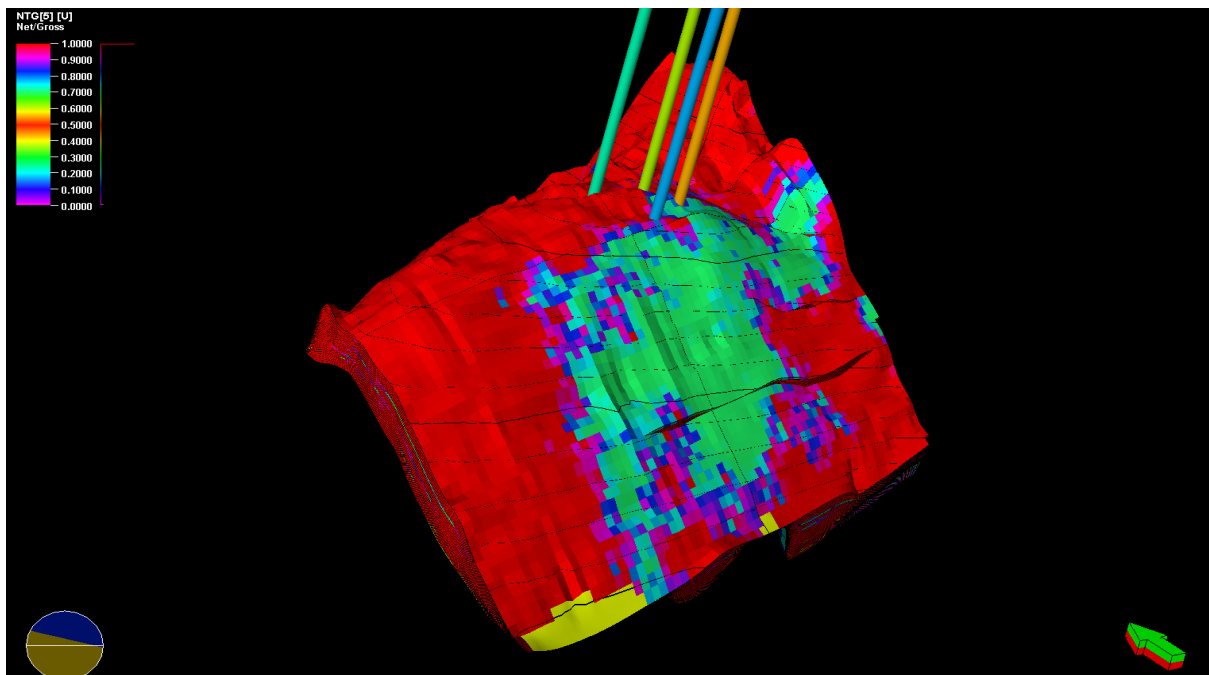


Figure 23: Net-To-Gross model generated for reservoir R_3000

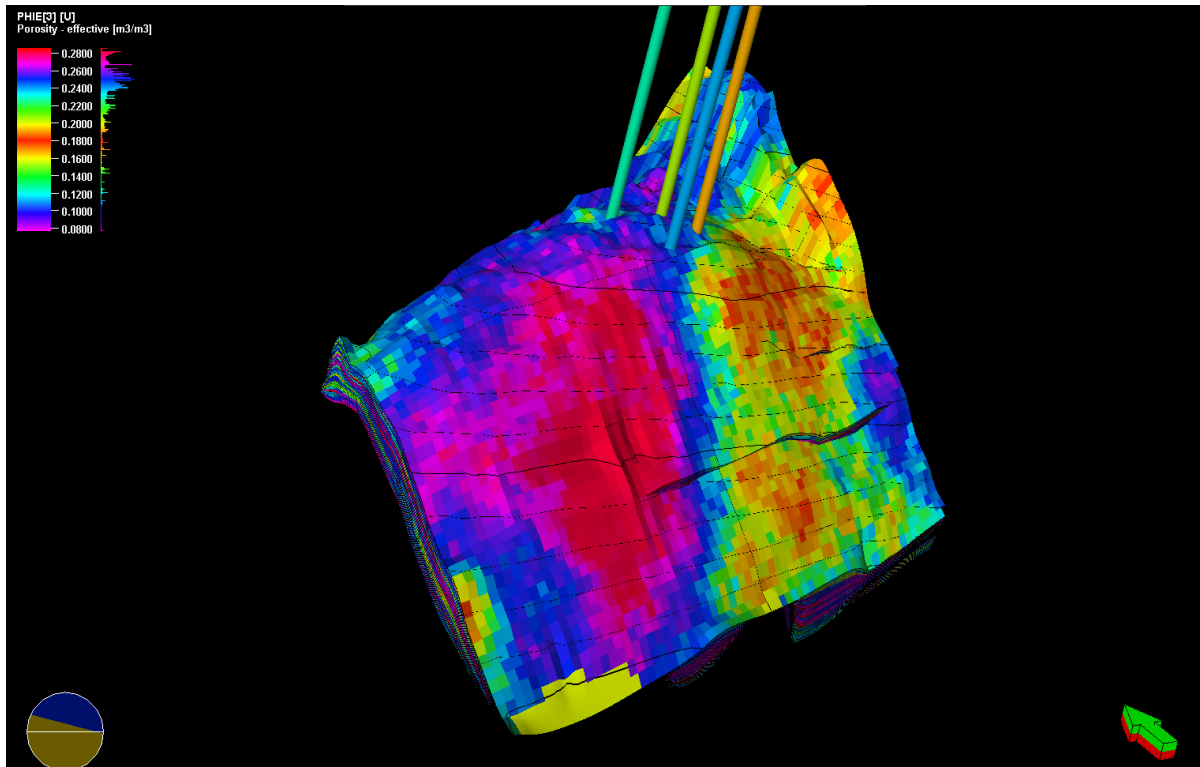


Figure 24: Effective porosity model generated for reservoir R_3000

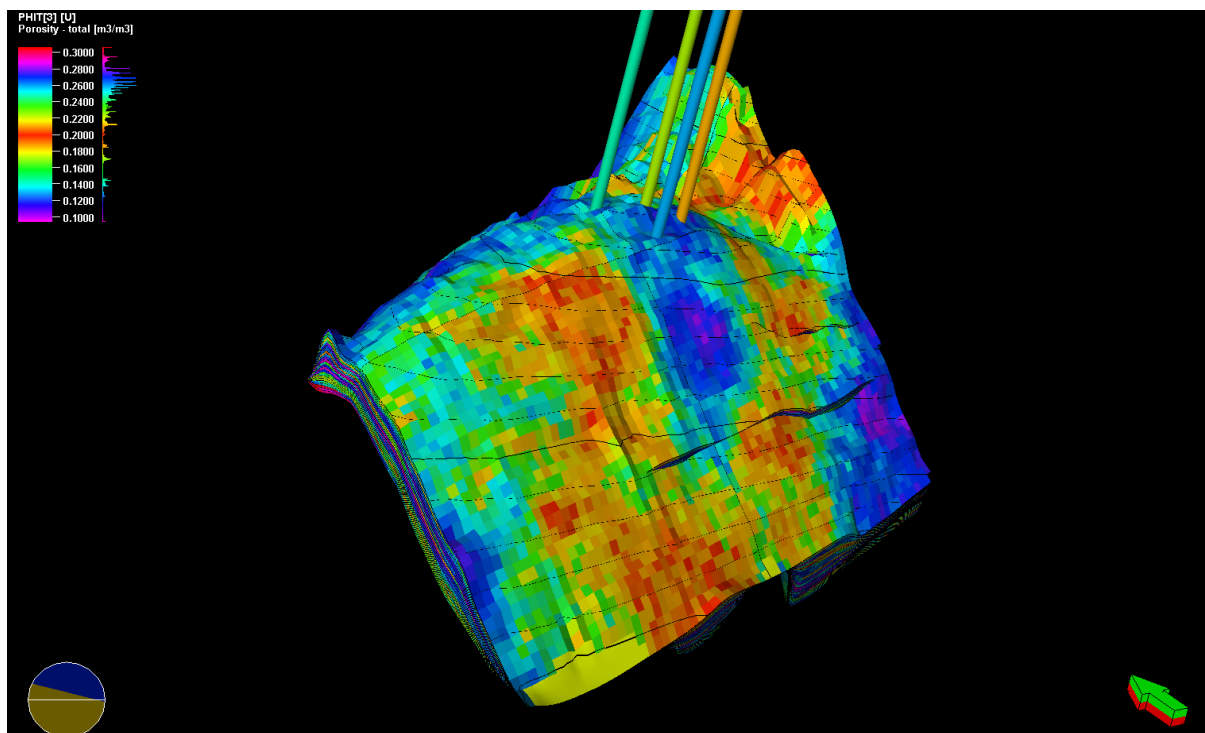


Figure 25: Total porosity model generated for reservoir R_3000

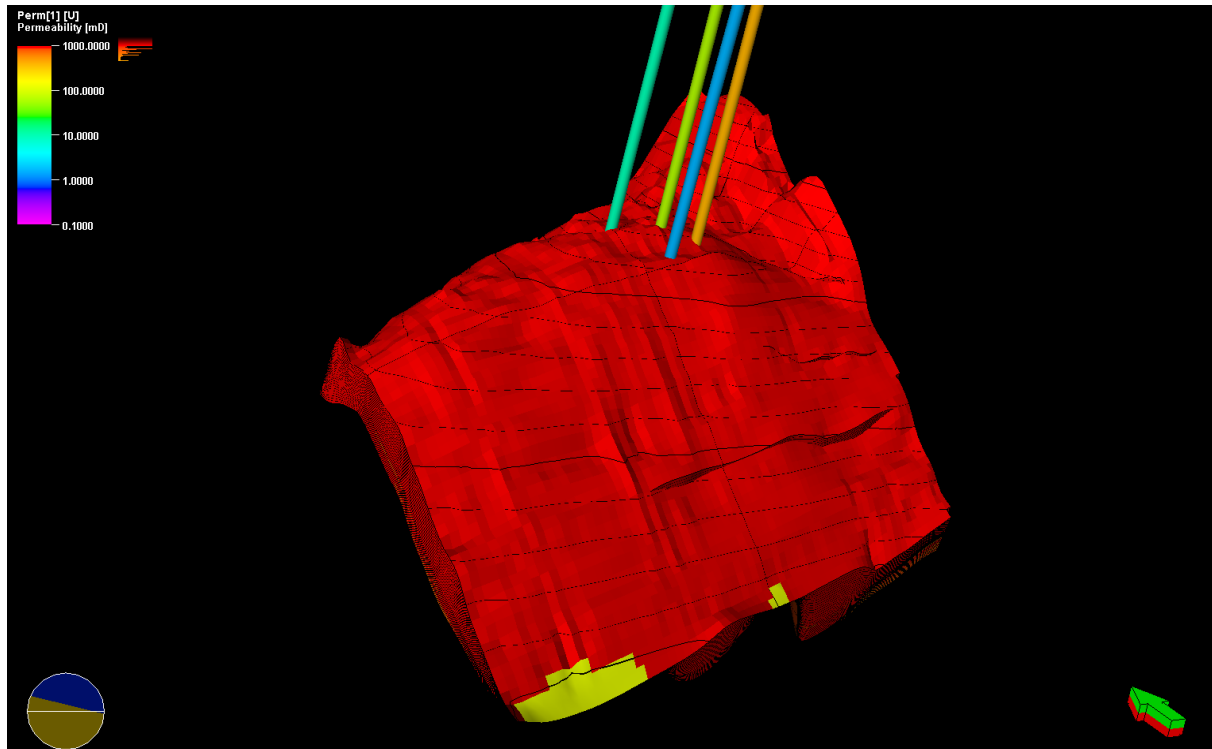


Figure 26: Permeability model generated for reservoir R_3000

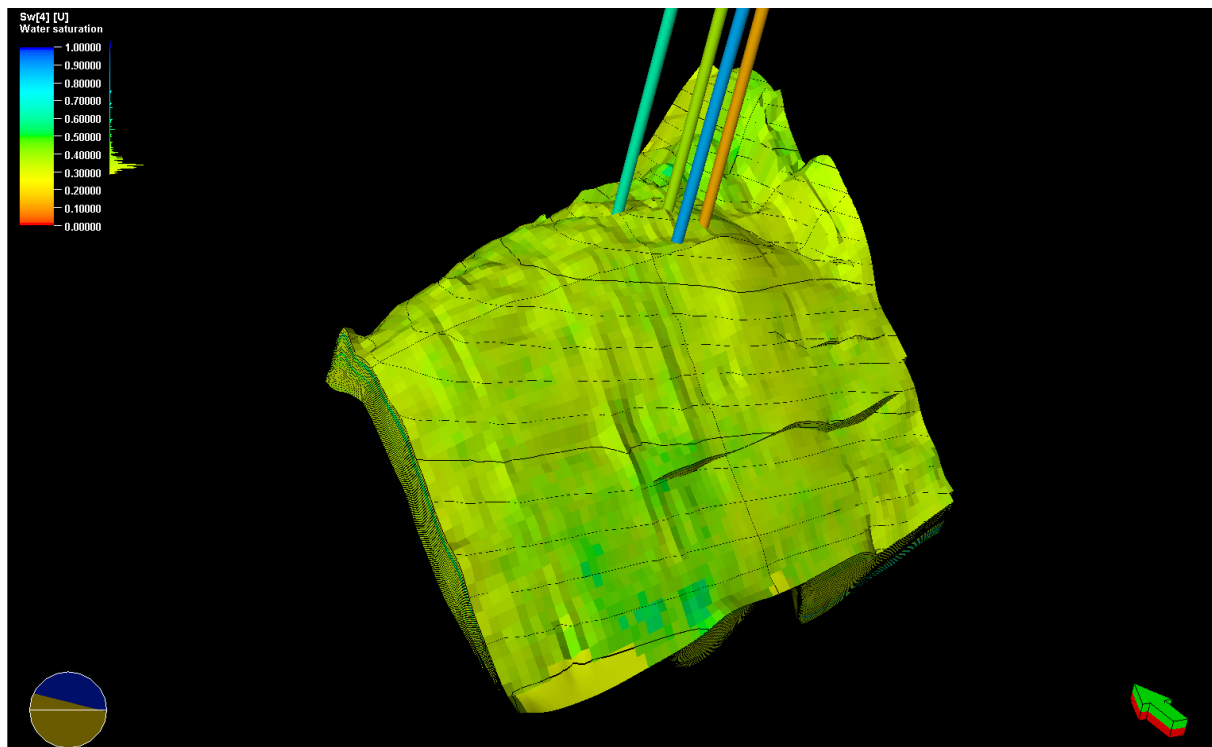


Figure 27: Water saturation model generated for reservoir R_3000

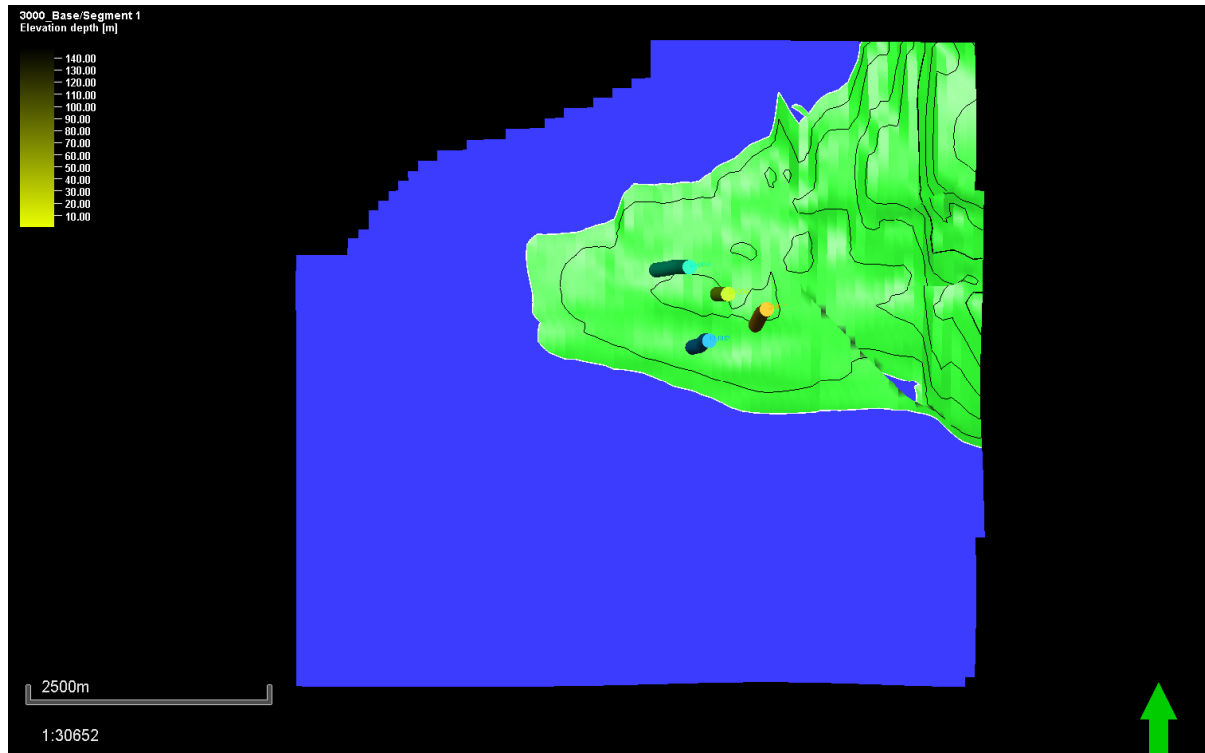


Figure 28: OWC delineating oil and water (brine) zones for reservoir R_3000

Item	\$Recoverable_oil_10_6_sm3_	\$STOIP_in_oil_10_6_sm3_	\$Pore_volume_10_6_rm3_	\$Net_volume_10_6_m3_	\$HCPV_oil_10_6_rm3_	\$Bulk_volume_10_6_m3_
Case1	1.6863019429407	1.6863019429407	4.98768084246715	22.7790824413482	2.78239816564758	290.436682528834
Case2	0.933534975422577	0.933534975422577	2.62105595377693	12.490742555204	1.54033268719004	290.436682528835
Case3	1.55699412533478	1.55699412533478	3.39428715928752	15.7123464526275	2.56904026968076	290.436682528834
Case4	2.03586580365404	2.03586580365404	5.80347537089749	26.6370986798018	3.35917852749034	290.436682528835
Case5	2.03586580365404	2.03586580365404	5.80347537089748	26.6370986798018	3.35917852749034	290.436682528835

Figure 29: STOIP values simulated for five case scenarios in reservoir R_3000

3.5. Discussion

Hydrocarbon bearing zones has been delineated and evaluated for their reservoir of interest, as well as the fluid and water contact determined. 3-D models of the reservoir structure, fluid contact, porosity and permeability, and fluid saturation has shown that the delineated reservoirs have economic value. The reservoir of interest was penetrated at depths 3180.75 – 3258.56 m, 3135.84 – 3259.90 m, 3142.54 – 3275.76 m and 3205.08 – 3283.56 m, across the wells.

The model reveals that NTG is between 70 - 88%, while the result from the petrophysical analysis indicates the field average of 79%, which is an indication of a probable hydrocarbon zone. The water saturation evaluated from the model ranges between 40% - 60%, while the petrophysical analysis indicates that the field average is 58.5%, zones with water saturation above 58 percent were considered as aquifer zones. The hydrogen saturation generated model ranges between 18 - 65%, while the petrophysical analysis field average is 41.5%. Investigation of the permeability model revealed reservoir permeability above 1000md and result from the petrophysical analysis indicates that the field average is 1570.649 md. Therefore, high reservoir deliverability is expected within the producing zone of the reservoir since hydrocarbon pore volume is very good. Investigation of the porosity model revealed a range of porosity 27m³/m³ and result from the petrophysical analysis indicates that the field average is 25 m³/m³, this values indicating possible hydrocarbon pore volume with well interconnected pore spaces and water-wet reservoir rocks, which permit high reservoir deliverability. These values suggest a reservoir with reserves considerably viable for economic production, having estimated stock tank oil initially in place (STOIP) of 1.4245 MMstb for the reservoir.

4. Conclusion

The petrophysical analysis showed that the five reservoirs units delineated were of good reservoir quantities as the effective and total porosities were high, with good permeability and low water saturation. From the result of

this study, the petrophysical analysis indicates that the field average Net to Gross (NTG), water saturation (S_w), permeability and porosity are 79%, 58%, 14245.50mD and 23% respectively. 3D static model was constructed from the input of the acquired data provided; the reservoir structures and shape were defined from the faults structures generated, while the addition of the structures to the boundaries aided the characterization of the formation top and base surfaces interpreted from the 3D seismic data. Faulting model, 3D pillar grid, horizon model, zoning, layering, property model, and petrophysical model deliverables all served as input in defining the constructed 3D geologic model. The analysis gave a better characterization of the field using the static modeling technique.

Acknowledgements

We wish to acknowledge the Department of Petroleum Resources, Shell Petroleum Development Company, Nigeria and DeGeoid Geosciences Limited, Rivers State, Nigeria for approving and releasing the data used for this research work. Special thanks to the Geophysics Research Unit of University of Port Harcourt, for resources, space and use of the unit facilities and personnel.

References

- Adeoti, L., Igiri, T., Adams, L., Adekunle, A., and Bello, M. A. (2014). Structural style and reservoir distribution in deep-water niger delta: a case study of "Nanny Field". *Br J Appl Sci Technol*, 4:1375–1391.
- Adiela. U.P A. O. and Omoboriowo, A. O. (2018). Depositional Environment and Petrophysical Studies of Ako Reservoir Sands, Niger Delta. *International Journal of Scientific Engineering and Science*, 2 (3): 5-10.
- Ailin J., Dongbo And Chengye, J. (2012). Advances and Challenges of Reservoir Characterization: A Review of The Current State-of-the-Art. *Intech Online Publisher, 51000 Rijeka, Croatia*.
- Aly, S. A. (1989). Evaluation of petrophysical properties of reservoir rocks using well logging analysis in Abu Ghyaradig Basin, Western Egypt. *Unpublished Ph.D. thesis, Faculty of science, kain Shams University, Cairo, Egypt*.
- Archie A.M. (1942) Method of water saturation estimation. *Department of Mining, Petroleum, and Geoscience Engineering, Shahrood University of Technology, Shahrood, Iran*, 5(2)
- Awe, T. A. (2017). Reservoir Characterization and Prediction of Reservoir Performance Using 3-D Static Modeling: Awe Field, Niger Delta, Nigeria. *International Basic and Applied Research Journal*, 3(8).
- Ezebialu, K. O., Ubituogwale, M. E., Odegua, E. A., Eche, E. U. and Sunebari, A. B. (2020). 3D Reservoir Modelling and Hydrocarbon Volume Estimation of "X" Field, Niger Delta, Nigeria. *International Journal of Research and Innovation in Applied Science (IJRIAS)*, V (II).
- Iyoha, A., Amadasunand, C. V. O. and Osemeikhian, J. E. A. . (2017). 3D Reservoir Modeling And Petrophysical Evaluation Of Oka Field Structure In The Eastern Niger Delta Basin, Nigeria. *Nigerian Annals Of Natural Sciences*, 16 (1) 048 – 056.
- Lukumon A., Njoku A., Olawale O. Julius F. and Musa B. (2014). Static Reservoir Modeling Using Well Log And 3-D Seismic Data In A KN Field, Offshore Niger Delta, Nigeria. *International Journal of Geosciences*, 4 (5): 93-106.
- Ogobodu, O. S. and Balogun, A.O. (2020). Application of 3-D Static Modeling and Seismic attribute analattribute analysis for Reservoir Characterization over Sobel-field Niger Delta, *International Journal of Engineering Science Invention (IJESI)*, 9 (1): 38-43
- Okoli, A. E., Agbasi, O. E., Lashin, A. A. and Sen, S. (2020). Static Reservoir Modeling of the Eocene Clastic Reservoirs in the Q-Field, Niger Delta, Nigeria. *Natural Resources Research*.
- Owolabi, O.O., Longjohn, T.F. and Ajenka J.A. (1994). An empirical expression for permeability in unconsolidated sands of eastern Niger Delta. *Journal of Petroleum Geology*. 17(1): 111-116.
- Shannon, P. M., and Naylor, N. (1989). "Petroleum Basin Studies London". *Graham and Trotman Limited*. 153-169.
- Short, K. C. and Stauble A. J. (1967). Outline of geology of Niger Delta. *American Association of Petroleum Geologists Bulletin*. 51: 761-779.
- Stacher, P. (1995). Present understanding of the Niger delta hydrocarbon habitat: Geology of Deltas. *AA Balkema, Rotterdam*, 257–267.
- Toba, A. A. (2017). Reservoir Characterization and Prediction of Reservoir Performance using 3-D Static Modelling: Awe Field, Niger Delta, Nigeria. *International Basic and Applied Research Journal*, 3(8): 1-17.
- Weber, K. and Daukoru E.M (1975). Sedimentological aspects of oil fields in Niger Delta. *Geologize en Mingbouw*, 50: 559-576.
- Weber, K. J. (1986). Hydrocarbon distribution patterns in Nigerian growth fault structures controlled by structural style & Stratigraphy. *Journal of Petroleum Science & Engineering*, 1: 91- 104.
- Wyllie, M. R. (1958). Sonic porosity. *American Association of Petroleum Geologists Bulletin*, 52.: 751-781.